https://doi.org/10.18502/jad.v20i3.22579

Original Article

Green Synthesis of Copper Oxide Nanoparticles Using Hydroalcoholic *Calotropis procera* Leaf Extract and Their in Vitro Antileishmanial Activity against *Leishmania tropica*

Alireza Salimi-Khorashad[1], Ehsan Salarkia[2], Seyed Mohammad Mousavi[3], Abbas Safdari-Adimi[1], Hadi Mirahmadi[4], *Ahmad Mehravaran[1]

[1]Infectious Diseases and Tropical Medicine Research Center, Research Institute of Cellular and Molecular Science in Infectious Diseases, Zahedan University of Medical Sciences, Zahedan, Iran
[2]Leishmaniasis Research Center, Kerman University of Medical Sciences, Kerman, Iran
[3]Research Center for Hydatid Disease in Iran, Kerman University of Medical Sciences, Kerman, Iran
[4]Clinical Immunology Research Center, Zahedan University of Medical Sciences, Zahedan, Iran

***Corresponding author:** Dr Ahmad Mehravaran, E-mail: ahmadmehravaran55@gmail.com

(Received 05 Aug 2026; accepted 31 Aug 2026)

Abstract

Background: Leishmaniasis remains a major public health concern due to treatment toxicity, prolonged regimens and emerging drug resistance. Green-synthesized metal oxide nanoparticles are promising candidates for alternative antileishmanial therapies. This study synthesized copper oxide nanoparticles (CuO NPs) using hydroalcoholic *Calotropis procera* leaf extract and evaluated their in vitro activity against *Leishmania tropica***.**

Methods: CuO NPs were synthesized using *C. procera* extract as a biological reducing and stabilizing agent and characterized by dynamic light scattering, field-emission scanning electron microscopy, energy-dispersive X-ray spectroscopy and Fourier-transform infrared spectroscopy. The antileishmanial activity of *C. procera* extract (CPE), CuO NPs, meglumine antimoniate (MA) and their combinations was assessed against promastigotes and intracellular amastigotes. Cytotoxicity was evaluated in THP-1-derived macrophages and selectivity indices (SI) were calculated. Apoptosis-related markers and oxidative stress parameters were also assessed.

Results: CuO NPs had a mean hydrodynamic diameter of 185.26±19 nm and a zeta potential of −15.93±2.6 mV. The CuO NPs+MA combination showed the strongest activity against amastigotes (IC_{50}= 52.19 µg/mL) and promastigotes (IC_{50}= 281.63 µg/mL), with a CC_{50} of 603.1 µg/mL and the highest SI (11.56). Treatment increased Bax, caspase-3, caspase-8 and ROS levels while reducing Bcl-2, SOD and CAT.

Conclusion: Green-synthesized CuO NPs, particularly in combination with MA, demonstrated promising antileishmanial activity and selectivity against *L. tropica*. These findings support further evaluation in vivo.

Keywords: Nanotechnology; Phytochemicals; *Leishmania* infections; Cupric oxide; Drug delivery systems

Introduction

Leishmaniasis is a major global problem that threatens millions of people living in tropical and subtropical regions of the world. The bite of an infected sandfly can transmit various species of the genus *Leishmania* and cause leishmaniasis in three main forms: cutaneous, visceral and mucocutaneous leishmaniasis (1). The disease particularly impacts underprivileged populations, with an estimated 700,000 to 1 million new cases annually, leading to significant morbidity and mortality in endemic regions. Current therapeutic options are limited by prolonged treatment duration, significant toxicity and emerging drug resistance (2).

The limitations associated with conventional anti-leishmanial therapies have intensified the demand for alternative treatment strategies. *Leishmania tropica* was selected in the present study because it is one of the principal causative agents of anthroponotic cutaneous

http://jad.tums.ac.ir
Published Online: September 30, 2026

Copyright © 2026 The Authors. Published by Tehran University of Medical Sciences.
This work is licensed under a Creative Commons Attribution-NonCommercial 4.0 International license (https://creativecommons.org/licenses/by-nc/4.0/). Non-commercial uses of the work are permitted, provided the original work is properly cited.

https://doi.org/10.18502/jad.v20i3.22579

leishmaniasis in Iran, particularly in southeastern and central endemic regions. Compared with other Iranian *Leishmania* species, especially *L. major*, *L. tropica* has shown a less favorable response to conventional pentavalent antimonial therapy, including meglumine antimoniate (Glucantime®). Clinical and experimental studies conducted in Iran during the last decade have reported reduced susceptibility, prolonged treatment duration, higher rates of treatment failure and the emergence of antimony-resistant *L. tropica* isolates. These characteristics make *L. tropica* a clinically relevant and challenging species for evaluating novel antileishmanial agents and combination therapies aimed at improving treatment efficacy while reducing drug toxicity (3–6). Many of the currently available drugs require prolonged administration, hospitalization and strict monitoring, while frequently inducing severe adverse effects such as cardiotoxicity, hepatotoxicity and nephrotoxicity. These drawbacks significantly reduce patient compliance and contribute to treatment failure (7). Given these limitations, there is intense research interest in developing alternative strategies, particularly those utilizing nanotechnology-based approaches. Nanoparticle-based therapeutics offer several advantages, including enhanced drug delivery, reduced toxicity and improved efficacy against resistant strains. Previous studies have demonstrated the potential of biogenic nanoparticles as promising antileishmanial agents; for example, Mohtasebi et al. reported significant in vitro and in vivo antiparasitic activity of biogenic antimony sulfide nanoparticles against *L. major* (8, 9, 10). Various nanoparticle-based delivery systems, including liposomes, archaeosomes, micelles, polymersomes and immune-stimulating complexes (ISCOMs), have emerged as powerful tools in biomedical research and infectious disease therapy, including for parasitic diseases like leishmaniasis (11–13).

Recent studies have emphasized plant extracts in green synthesis because of their efficiency and sustainability (10, 14). The green synthesis of metal oxide nanoparticles has gained considerable attention due to its simplicity, sustainability and ability to produce stable nanoparticles with controlled size and morphology (15, 16). Copper oxide nanoparticles (CuO NPs) specifically have shown remarkable potential in biomedical applications due to their unique physicochemical properties, including broad-spectrum antimicrobial, antifungal, and notably, antiparasitic activities (17, 18), making them a candidate of interest for anti-leishmanial applications.

Calotropis procera is a medicinal plant widely distributed in tropical and subtropical regions and represents a valuable biological resource for the green synthesis of metal nanoparticles. The leaves of this plant are rich in bioactive compounds, including flavonoids, alkaloids, phenolics and proteins, which facilitate the reduction and stabilization of metal ions during nanoparticle formation (17, 19–20). Beyond its direct antiparasitic activity, accumulating evidence indicates that *C. procera* can modulate host immune responses by enhancing oxidative stress pathways. In macrophages infected with *Leishmania*, the generation of reactive oxygen species (ROS) plays a pivotal role in parasite clearance, and plant-derived compounds have been shown to stimulate ROS production, thereby strengthening macrophage-mediated killing mechanisms (21–23).

Green-synthesized metal oxide nanoparticles derived from *Calotropis procera* leaf extracts exploit the plant's natural bioactive compounds to enhance antiparasitic activity. CuO nanoparticles produced through this approach exhibit favorable biological properties, including promising antimicrobial and antiparasitic potential (24). In *Leishmania*-infected macrophages, oxidative stress constitutes a key host defense mechanism, as activated macrophages produce free radicals and non-radical ROS like superoxide anions and H_2O_2, which exert cytotoxic effects on intracellular parasites. To counteract this, host cells express antioxidant enzymes like superoxide dismutase (SOD) and

http://jad.tums.ac.ir
Published Online: September 30, 2026

https://doi.org/10.18502/jad.v20i3.22579

catalase, which regulate ROS levels and protect cellular components.

Conversely, Leishmania parasites rely on a distinct thiol-based redox system, centered on trypanothione, to neutralize host-derived ROS and maintain intracellular survival. Therefore, disruption of this redox balance by enhancing ROS generation in macrophages or inhibiting parasite antioxidant enzymes can critically compromise parasite viability and, therefore, represents an attractive target for anti-leishmanial intervention. The present study aims to investigate this strategy by examining the effects of green-synthesized CuO NPs on redox status and apoptosis-related markers in the *L. tropica*-infected macrophage microenvironment, as an indirect indicator of anti-parasitic activity.

Materials and Methods

Experimental design and study flow

The study comprised five phases: (1) plant extract preparation; (2) green synthesis of CuO NPs (three independent batches); (3) characterization (DLS, FESEM-EDS, FTIR); (4) in vitro assays (anti-promastigote, anti-amastigote, cytotoxicity, apoptosis markers, ROS, SOD, CAT); (5) statistical analysis. Three biological replicates (each with 2–3 technical replicates) were performed. Treatment groups were tested in parallel (50–400 µg/mL). Randomization and blinding were applied. One-way ANOVA with Tukey's post hoc test was used. IC_{50}/CC_{50} values were calculated using probit regression analysis.

Synthesis of nanoparticles

Extraction from the plant

To prepare the hydroalcoholic extract, dried and powdered *C. procera* leaves were mixed with an 80:20 ethanol-water solution and stirred for 24 hours. Following initial filtration and passage through Whatman No. 4 filter paper, the collected extracts were concentrated to dryness under reduced pressure at 40 °C using a rotary evaporator. The resulting dried materials were preserved at 4 °C for subsequent analyses.

Preparation of copper oxide nanoparticles by green synthesis method

CuO NPs were synthesized by reacting the plant extract with a 1 mM $CuCl_2$ solution overnight at 37 °C. The resulting NPs were pelleted via centrifugation, washed with distilled water and dried. The aqueous extract acted as a dual-purpose reducing agent and solvent. The purified nanoparticles were then prepared in aqueous suspension for further analysis. All experiments were performed using three independently synthesized batches of CuO NPs.

Colloidal System analysis: size distribution and surface charge

Dynamic light scattering was employed to evaluate the physical characteristics of biosynthesized copper oxide nanoparticles in aqueous medium. Hydrodynamic diameter, polydispersity index and zeta potential were quantitatively determined. The analysis was carried out at 25 °C using a Malvern Zetasizer instrument, for which the nanoparticle colloid was diluted with deionized water before measurement.

Physicochemical characterization of synthesized nanoparticles

A field emission scanning electron microscope (KYKY EM8000F, China) was utilized to investigate the structural and compositional features of biologically synthesized copper oxide nanoparticles. Key parameters including surface texture, particle dispersion and elemental integrity were analyzed. Specimens were prepared by transferring a dilute colloidal solution onto a silicon substrate via droplet deposition and subsequent solvent evaporation under ambient conditions. Energy Dispersive X-ray Spectroscopy (EDS), coupled with the FESEM instrument, facilitated the identification of elemental constituents.

http://jad.tums.ac.ir
Published Online: September 30, 2026

https://doi.org/10.18502/jad.v20i3.22579

Fourier transform infrared spectroscopy for surface functionality assessment

The presence of surface-anchored organic moieties derived from the plant extract on the biosynthesized CuO NPs was verified via Fourier Transform Infrared Spectroscopy (FTIR) coupled with an Attenuated Total Reflectance setup. Specimens were prepared by depositing a minute quantity of desiccated nanopowder onto the ATR stage, followed by the application of controlled force via the built-in press to achieve optimal surface adhesion. Spectral acquisition spanned the 400–4000 cm^{-1} wavenumber region.

In vitro experiments

The concentration range of 50–400 µg/mL was selected based on preliminary dose-finding experiments and previous literature on green-synthesized nanoparticles against *Leishmania*. The same range was used for all interventions to allow direct comparison. The combination studies were designed to explore additivity/synergy and to reduce the effective dose of meglumine antimoniate (MA).

Parasite culture

Promastigote forms of *L. tropica* (strain MHOM/IR/Mash2) were propagated in RPMI-1640 medium enriched with 10% fetal bovine serum (Gibco, USA) and 1% penicillin-streptomycin solution. Cultures were incubated at 25±1 °C with routine passaging every 72–96 hours.

Monocyte-to-macrophage differentiation protocol

The THP-1 human monocytic cell line was obtained from the Pasteur Institute of Iran. Cells were cultured in DMEM medium supplemented with 10% FBS and 1% penicillin-streptomycin under humidified conditions (37 °C, 5% CO_2). Differentiation into macrophage-like cells was achieved through 24-hour incubation with 100 nM phorbol 12-myristate 13-acetate.

Anti-promastigote assay

Promastigote viability was evaluated using an MTT assay. Briefly, *L. tropica* promastigotes (1×10^5/mL) were incubated in 96-well plates with serially diluted test compounds (CuO NPs, CPE, MA, alone or combined) for 72 h at 25 °C. After adding MTT (10 µL of a 5 mg/mL stock) and incubating for 3 h, formazan crystals were dissolved with DMSO (100 µL/well). Absorbance was measured at 540–570 nm using a microplate reader and inhibition (%) was calculated relative to the untreated control. (CPE: *C. procera* extract, MA: meglumine antimoniate). The plate layout for treatment groups was randomized, and the investigator was blinded during absorbance measurement. Inhibition (%)= (1– absorbance treated/absorbance control)× 100.

Anti-amastigote assay

For the infection assay, THP-1-derived macrophages (1×10^5 cells/well on coverslips) were infected with *L. tropica* promastigotes (MOI 10:1) for 24 h. After removing extracellular parasites, infected cells were treated with serial concentrations (50–400 µg/mL) of MA, CuO NPs, CPE, or combined formulations for 72 h. Coverslips were then fixed (methanol), stained (Wright–Giemsa), and examined by light microscopy. Amastigotes were counted in ≥ 100 macrophages per condition, and results are presented as the infection index (mean amastigotes/macrophage). Counting of infected macrophages and amastigotes was performed by an investigator blinded to the treatment groups. Infection index= (number of infected macrophages/total macrophages counted) × (mean number of amastigotes per infected macrophage).

Quantitative assessment of apoptotic markers in infected macrophages

Protein expression levels of apoptosis-associated factors including Bax, Bcl-2, caspase-3 and caspase-8 were determined in *L. tropica*-infected THP-1-derived macrophages

https://doi.org/10.18502/jad.v20i3.22579

harboring intracellular amastigotes. Commercial ELISA kits (Bax: E-EL-H0562; Bcl-2: E-EL-H0114, ElabScience, USA; caspase-3: ABIN3044699; caspase-8: ABIN3044700, Picokine, USA) were employed following manufacturer recommendations. For transcriptional analysis, total RNA was isolated using TRIzol reagent and reverse-transcribed into cDNA using a commercial synthesis kit (both sourced from Yekta Tajhiz Azma, Iran). Quantitative real-time PCR was conducted on a Rotor-Gene Q platform (Qiagen) utilizing SYBR Green Master Mix, gene-specific primers (detailed in Table 1) and cDNA templates. Target gene expression levels, normalized to the GAPDH housekeeping gene, were calculated employing the 2^(-ΔΔCt) relative quantification method.

Quantification of oxidative stress parameters and antioxidant activities

THP-1 macrophages infected with *L. tropica* amastigotes were collected, rinsed twice with ice-cold PBS, and lysed for downstream assays. Intracellular ROS were measured via the KPG ROS detection kit (Karmania Pars Gene, Iran). Cell lysates were incubated with the provided probe in 96-well plates, followed by absorbance measurement at 450 nm. ROS levels were calculated as fold change relative to untreated controls (set as 1).

Superoxide dismutase and catalase activities were assessed using the Nasdox™ and Nactaz™ kits (Navform, Iran), respectively, following manufacturer instructions. Enzyme activities were expressed as relative values compared to the control group.

Statistical analysis

All experiments were performed in three biological replicates, with technical replicates as indicated per assay. Normality was assessed using the Shapiro–Wilk test, and homogeneity of variances by Levene's test. For multiple-group comparisons, one-way ANOVA followed by Tukey's post hoc test was used. For two-group comparisons, a two-tailed unpaired Student's t-test was applied. IC_{50} and CC_{50} values were calculated using probit regression (SPSS v26). A p-value< 0.05 was considered statistically significant. GraphPad Prism 9 was used for graph preparation.

Results

Characteristics of produced nanoparticles Dynamic Light Scattering (DLS)

The nanoparticles exhibited an average hydrodynamic diameter of 185±19 nm with a zeta potential of -15.93±2.6 mV. The relatively high PDI indicates a broad particle size distribution and some degree of heterogeneity (Table 2).

Field-emission scanning electron microscopy-based morphological and elemental characterization

Surface features, particle geometry and elemental profile of the biosynthesized CuO NPs were investigated via field-emission scanning electron microscopy. Micrographs (Fig. 1) corroborated the size distribution obtained from DLS and demonstrated predominantly spherical particle morphology. Some degree of polydispersity and agglomeration was also observed.

Fourier transform infrared analysis: surface functionality and biofabrication confirmation

The involvement of phytochemicals in the reduction and capping of CuO NPs was verified via Fourier transform infrared spectroscopy (Fig. 2). A broad O–H stretching band around 3255 cm^{-1} pointed to phenolic moieties or surface-adsorbed water derived from the botanical extract. Signals at 2919 cm^{-1} and 1043 cm^{-1} were assigned to aliphatic C–H and C–O stretching modes, respectively. Absorptions near 1604 cm^{-1} and 1412 cm^{-1} originated from carbonyl stretching and aromatic C–C vibrations, characteristic of flavonoid/polyphenolic structures. Crucially, the distinct Cu–O stretching band below 700 cm^{-1} (~521

http://jad.tums.ac.ir
Published Online: September 30, 2026

https://doi.org/10.18502/jad.v20i3.22579

cm^{-1}) confirmed the successful formation of copper oxide nanoparticles. The detection of plant-derived organic residues on the particle surface corroborates their dual function as reducing and capping agents.

In vitro assessments

Anti-promastigote functions

The direct effect of CPE, green-synthesized CuO NPs, MA and their combinations on the viability of *L. tropica* promastigotes was evaluated after 72 h of treatment. As shown in Fig. 3, all treatments reduced parasite viability in a concentration-dependent manner compared to the untreated control. The combination of CuO NPs with MA (CuO NPs+MA) exhibited the most potent anti-promastigote activity, resulting in the lowest IC_{50} value (see Table 3). These results demonstrate the direct leishmanicidal potential of the green-synthesized CuO NPs and their synergistic effect with the standard drug.

Anti-amastigote activity and cytotoxicity assessment

The anti-amastigote activity of the treatments was evaluated in *L. tropica*-infected THP-1 macrophages. All treatments significantly and dose-dependently reduced the intracellular parasite burden compared to the untreated control (Table 3). The combination therapies (CPE+MA and CuO NPs+MA) were the most potent, with higher concentrations achieving near-complete elimination. Cytotoxicity against uninfected THP-1 macrophages was assessed to determine treatment selectivity. The half-maximal cytotoxic concentration (CC_{50}) and the derived selectivity index (SI) are presented in Table 4. All formulations showed CC_{50} values markedly higher than their corresponding anti-amastigote IC_{50} values, yielding SI > 1 and confirming a selective anti-leishmanial effect. Notably, the CuO NPs+MA combination yielded the highest SI value.

Apoptotic mediators

The induction of apoptosis was assessed by measuring key regulatory markers at both the protein (ELISA) and gene expression (RT-qPCR) levels (Fig. 4). Compared to untreated controls and single-agent treatments, the combination therapies (CPE+MA and CuO NPs+MA) significantly increased the protein levels of the pro-apoptotic factors Bax, Caspase-3 and Caspase-8, while decreasing the anti-apoptotic protein Bcl-2. A corresponding transcriptional response was observed, with the same combinations markedly upregulating Bax, Caspase-3 and Caspase-8 mRNA and downregulating Bcl-2 mRNA. The most pronounced modulation across all markers occurred in the CuO NPs+MA treatment group.

ROS, SOD and catalase in amastigotes

Oxidative stress was evaluated in intracellular amastigotes by measuring ROS levels and the activities of the antioxidant enzymes SOD and CAT (Fig. 5). All single treatments (CPE, CuO NPs, MA) significantly increased ROS production compared to the untreated control. This effect was markedly enhanced in the combination groups (CPE+MA and CuO NPs+MA), with the CuO NPs+MA combination inducing the highest ROS levels. Conversely, SOD and CAT activities were significantly reduced in all treated groups, with the most pronounced decrease observed in the combination treatments, particularly CuO NPs+MA.

http://jad.tums.ac.ir
Published Online: September 30, 2026

https://doi.org/10.18502/jad.v20i3.22579

Table 1. Primer sequences and amplicon sizes of apoptosis-related genes (Bax, Bcl-2, Caspase-3 and Caspase-8) and the reference gene glyceraldehyde-3-phosphate dehydrogenase (GAPDH) used for quantitative real-time PCR (qRT-PCR) analysis of gene expression in macrophages

Template	Forward and reverse sequences (5^0-3^0)		Product size (bp)
Bax	Forward	CCCGAGAGGTCTTTTTCCGAG	155
	Reverse	CCAGCCCATGATGGTTCTGAT	
Bcl2	Forward	GGTGGGGTCATGTGTGTGG	89
	Reverse	CGGTTCAGGTACTCAGTCATCC	
Caspase 3	Forward	CATGGAAGCGAATCAATGGA	59
	Reverse	CTGTACCAGACCGAGATGTCA	
Caspase 8	Forward	AGAGTCTGTGCCCAAATCAA	59
	Reverse	CTGCTTCTCTCTTTGCTGAA	
GAPDH	Forward	AGGTCGGTGTGAACGGATTTG	95
	Reverse	GGGGTCGTTGATGGCAACA	

Table 2. Physicochemical characteristics of green-synthesized nanoparticles in aqueous suspension after synthesis, including hydrodynamic size, zeta potential and polydispersity index (PDI). Data are presented as mean ± standard deviation (SD; n= 3)

Formulation	Size(nm)	Zeta(mV)	PDI
Green synthesized NPs	185.26 ± 19	−15.93 ±2.6	0.951±0.01

Table 3. Effects of different concentrations of Tween 80 solution (TS), meglumine antimoniate (MA), chitosan–plant extract formulation (CPE), copper oxide nanoparticles (CuO) and their combinations on the mean number of intracellular amastigotes in infected macrophages. Amastigote burden was assessed following treatment at the indicated concentrations and compared with the untreated control group (UC). Data are presented as mean ± standard deviation (SD), and P values indicate comparisons with the untreated control

Concentration (µg/ml)	MA	P Value	TS	P Value
0 (UC)	54.3±3.8	-	54.3±3.8	-
50	41.2±2.1	<0.001	52.2±2.2	>0.05
100	22.4±4.1	<0.001	49.1±3.0	>0.05
200	15.1±1.2	<0.001	45.3±2.8	>0.05
400	0.0±0.0	<0.001	43.3±4.6	>0.05
Concentration (µg/ml)	CPE	P Value	CPE+MA	>0.05
0 (UC)	54.3±3.8	-	54.3±3.8	-
50	48.3±2.5	<0.001	34.5±2.6	<0.001
100	34.2±4.5	<0.001	16.2±0.8	<0.001
200	18.6±1.2	<0.001	3.2±0.2	<0.001
400	11.4±0.6	<0.001	0.0±0.0	<0.001
Concentration (µg/ml)	CuO	P Value	CuO+MA	P Value
0 (UC)	54.3±3.8	-	54.3±3.8	-
50	40.3±2.9	<0.001	27.9±1.4	<0.001
100	26.2±4.6	<0.001	15.1±0.9	<0.001
200	15.5±2.1	<0.001	0.0±0.0	<0.001
400	0.0±0.0	<0.001	0.0±0.0	<0.001

http://jad.tums.ac.ir
Published Online: September 30, 2026

https://doi.org/10.18502/jad.v20i3.22579

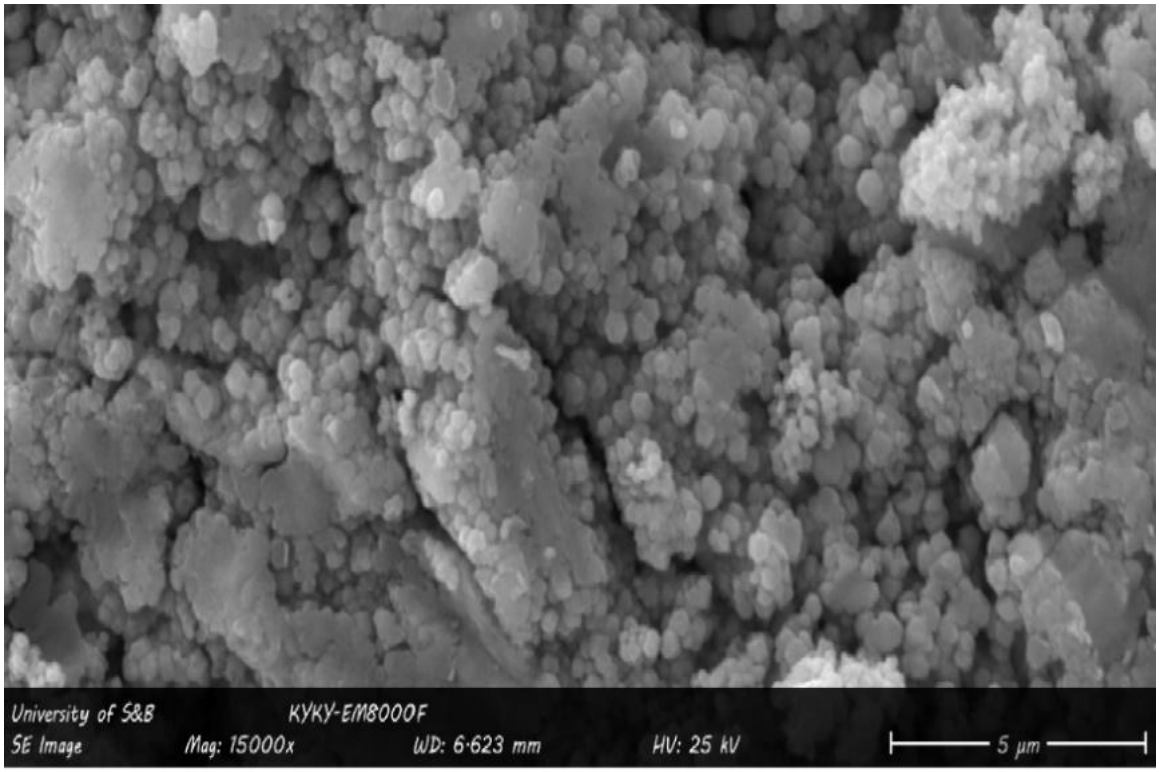


Fig. 1. Scanning electron microscopy of green-synthesized copper oxide nanoparticles (CuO NPs) showing surface morphology and aggregation; 15,000× magnification, 25 kV, scale bar: 5 µm

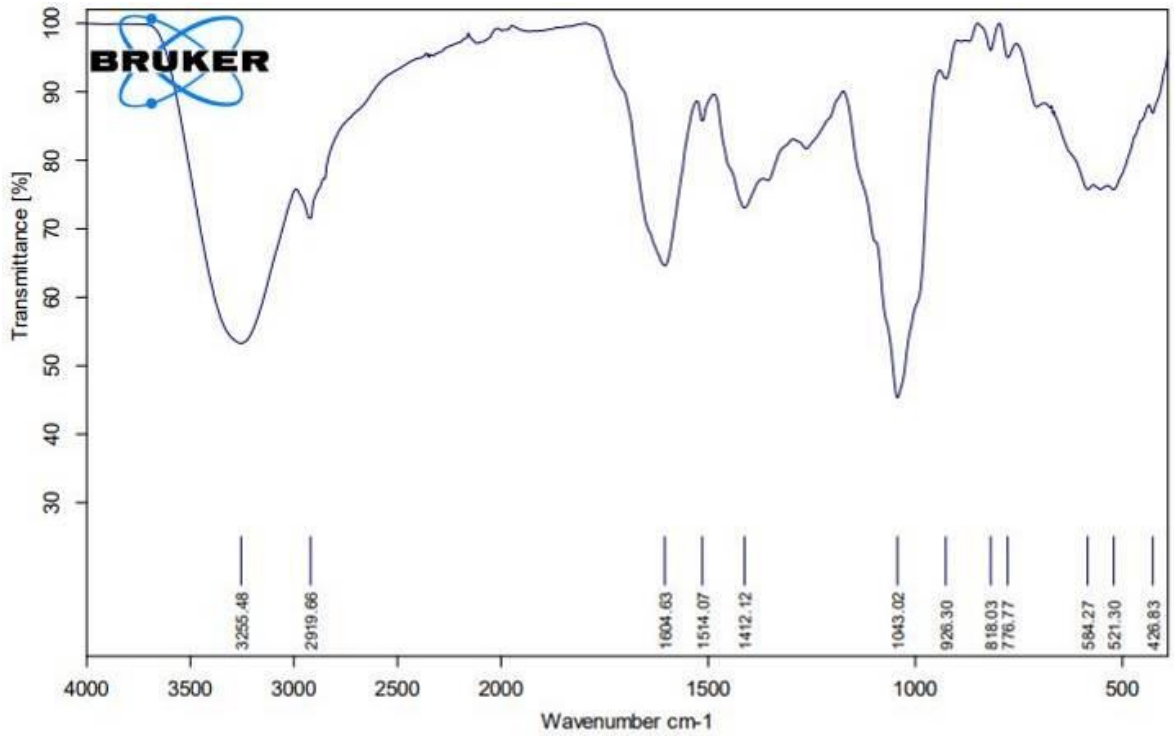


Fig. 2. Schematic representation of the FTIR technique used for green synthesized copper oxide nanoparticles (CuO NPs) analysis

http://jad.tums.ac.ir
Published Online: September 30, 2026

https://doi.org/10.18502/jad.v20i3.22579

Table 4. Evaluation of IC_{50} values for CS, MA, CuO and their combination against promastigotes and amastigotes of *Leishmania tropica*, compared to MAT and CC_{50} values of drugs on macrophages to calculate the selectivity index (SI)

	IC_{50} Amastigotes	*P* Value	IC_{50} Pro-mastigotes	*P* Value	CC_{50} Macro-phages	Selective Index
MA	96.66	-	334.95	-	693.3	7.17
TS	1249.66	<0.001	3346.2	<0.001	6673.4	5.34
CPE	141.14	<0.001	393.15	<0.001	762.3	5.40
CPE+MA	66.01	<0.001	312.46	<0.001	655.1	9.92
CuO NPs	109.17	<0.001	329.68	<0.001	689.7	6.32
CuO NPs+MA	52.19	<0.001	281.63	<0.001	603.1	11.56

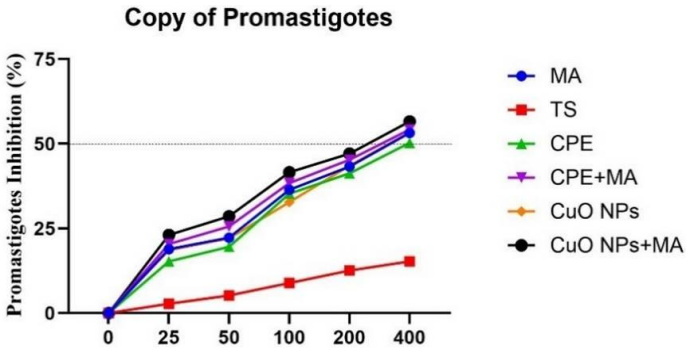


Fig. 3. In vitro anti-promastigote activity of the tested formulations against *Leishmania tropica* after 72 h of exposure. Promastigotes were treated with meglumine antimoniate (MA), *Calotropis procera* leaf extract (CPE), green-synthesized copper oxide nanoparticles (CuO NPs), or their combinations (0–400 µg/mL). Tween 80 (TS) was used as the vehicle control at the corresponding concentration. Parasite viability was determined by MTT assay and expressed as mean ± SD (n= 3)

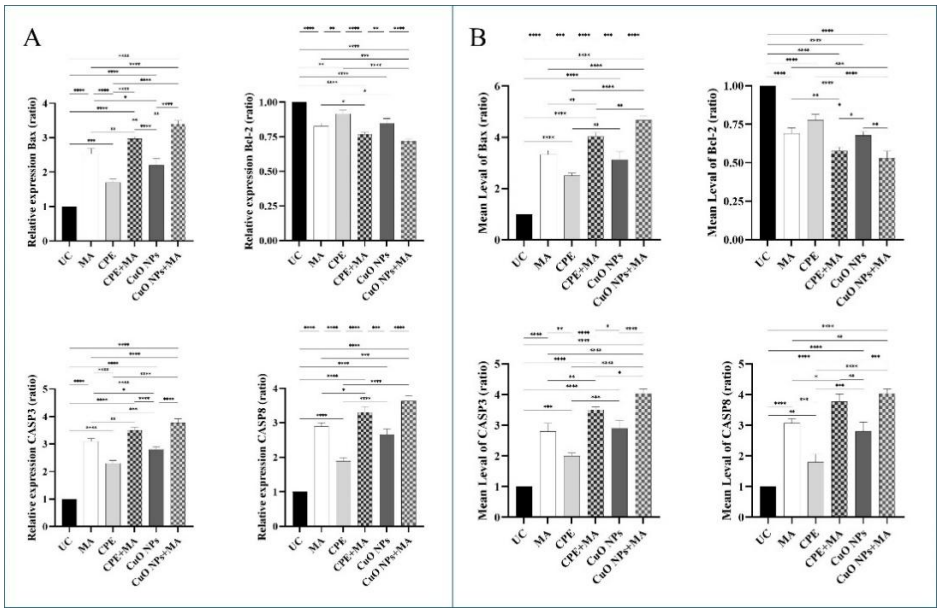


Fig. 4. Effect of the treatments on apoptosis-related markers in *Leishmania tropica*-infected THP-1 macrophages after 72 h. Cells were treated with meglumine antimoniate (MA), *Calotropis procera* leaf extract (CPE), copper oxide nanoparticles (CuO NPs), or their combinations. (A) Relative mRNA expression levels of Bax, Bcl-2, Caspase-3 and Caspase-8 were determined by RT-qPCR. (B) Corresponding protein levels measured by ELISA. Data are presented as mean ± SD from three independent biological replicates (each with two technical replicates). Statistical analysis was performed using one-way ANOVA followed by Tukey's post hoc test. *P< 0.05, **P< 0.01, ***P< 0.001 versus the untreated control

http://jad.tums.ac.ir
Published Online: September 30, 2026

https://doi.org/10.18502/jad.v20i3.22579

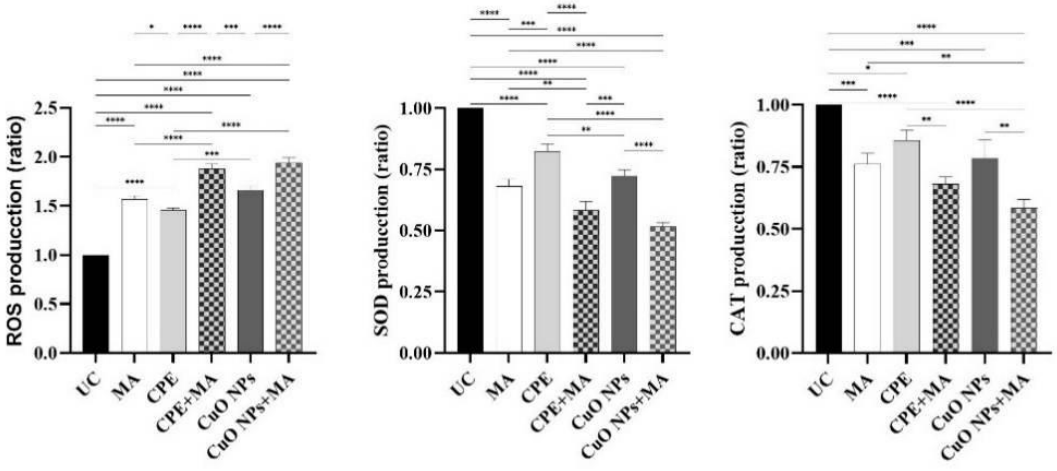


Fig. 5. Intracellular oxidative stress parameters in *Leishmania tropica-infected* THP-1 macrophages following treatment. Infected cells were exposed to meglumine antimoniate (MA), *Calotropis procera* leaf extract (CPE), copper oxide nanoparticles (CuO NPs), or their combinations. Intracellular reactive oxygen species (ROS) levels and the activities of superoxide dismutase (SOD) and catalase (CAT) were measured in cell lysates and expressed relative to the untreated control (set to 1). Data are presented as mean ± SD from three independent biological replicates. Statistical analysis was performed using one-way ANOVA followed by Tukey's post hoc test. *P< 0.05, **P< 0.01, ***P< 0.001 versus the untreated control

Discussion

Leishmaniasis remains a formidable global health burden, with current therapeutic regimens often compromised by escalating drug resistance, severe side effects and complex administration protocols that hinder patient compliance in endemic regions (2, 7). This pressing clinical landscape has catalyzed the exploration of innovative strategies, among which nanotechnology holds significant promise. Nanoparticles can enhance drug bioavailability, target parasitic reservoirs, and potentially overcome resistance mechanisms (9, 10). Within this paradigm, green synthesis utilizing biological resources as nanofactories has emerged as a superior alternative to conventional physicochemical methods, offering a route that is not only environmentally benign but also yields biocompatible and functionally rich nanostructures (15, 25). This study was therefore designed to synthesize and characterize copper oxide nanoparticles (CuO NPs) using the leaf extract of *Calotropis procera* and to rigorously evaluate their anti-leishmanial potential against *Leishmania tropica*.

Calotropis procera was selected as a bioresource due to its well-documented pharmacognostic profile, rich in flavonoids, alkaloids, phenolics and proteins that possess inherent reducing and stabilizing capabilities (17, 19–20). Our successful synthesis of CuO NPs underscores the efficacy of the leaf extract as a versatile nanofactory. The characterization data robustly confirm the formation of nanoparticles. Dynamic Light Scattering (DLS) revealed an average hydrodynamic diameter of 185.26± 19 nm and a negative zeta potential (-15.93± 2.6 mV), parameters indicative of a moderately stable colloidal suspension with a low propensity for uncontrolled aggregation (Table 2). The spherical morphology observed via field emission scanning electron microscopy (FESEM) (Fig. 1) is consistent with numerous reports on plant-mediated synthesis and provides a high surface-area-to-volume ratio beneficial for biological interactions (10). Fourier transform infrared spectroscopy (FTIR) analysis provided critical insights into the synthesis mechanism (Fig. 2). The spectrum displayed

http://jad.tums.ac.ir
Published Online: September 30, 2026

https://doi.org/10.18502/jad.v20i3.22579

characteristic absorption bands for O–H stretching (~3255 cm^{-1}), C–H stretching (~2919 cm^{-1}) and C–O stretching (~1043 cm^{-1}), all signature peaks of the phytochemicals present in *C. procera* extract (26). Crucially, the distinct peak observed below 700 cm^{-1} (at ~521 cm^{-1}) is unequivocally attributed to the Cu–O vibrational mode, confirming the formation of copper oxide crystals (10). The co-existence of plant-derived and metal oxide peaks strongly suggests that phytoconstituents are not merely facilitators of reduction but also form a stabilizing corona around the NPs, potentially dictating their biological interface.

The anti-leishmanial efficacy of the green-synthesized CuO NPs was pronounced and dose-dependent against both the extracellular promastigote and the clinically relevant intracellular amastigote forms of *L. tropica* (Fig. 3, Tables 3 and 4). This dual-stage activity is of paramount importance, as a successful therapeutic agent must eradicate the motile infective stage (promastigote) and, more critically, eliminate the sheltered intracellular amastigote responsible for chronic infection. The observed activity aligns with and extends the known pharmacologic potential of *C. procera*. While Ilaghi et al. (27) demonstrated that the crude extract itself has activity against *L. tropica*, our work advances this finding by demonstrating that the extract's value can be amplified through its use in fabricating nanostructures with enhanced properties. Furthermore, a notable finding was the synergistic interaction between CuO NPs and the standard drug meglumine antimoniate (MA). The combination therapy (CuO NPs+MA) consistently showed superior parasite suppression compared to either agent alone. This synergy mirrors emerging trends in nanomedicine for infectious diseases, where, for example, Majeed et al. (28) reported enhanced efficacy of MA when combined with green-synthesized silver nanoparticles. This suggests that our CuO NPs may sensitize the parasite to the conventional drug or act through complementary pathways, a strategy that could lower the effective dose of MA and mitigate its associated toxicity.

To elucidate the mechanistic basis of the leishmanicidal effect, we investigated markers of apoptosis and oxidative stress, two interrelated pathways often triggered by metal oxide nanoparticles (29). Our data compellingly show that treatment, particularly with the CuO NPs+ MA combination, induced a pro-apoptotic state in the parasites. This was evidenced by a significant increase in the protein and gene expression of the executioner caspases (Caspase-3, Caspase-8) and the pro-apoptotic regulator Bax, concurrent with a decrease in the anti-apoptotic protein Bcl-2 (Fig. 4). Parallel to this, we observed a profound disruption of the parasite's redox homeostasis. Treated amastigotes exhibited a surge in intracellular reactive oxygen species (ROS) alongside a significant decline in the activity of key antioxidant defense enzymes, superoxide dismutase (SOD) and catalase (CAT) (Fig. 5). *Leishmania* parasites are particularly susceptible to oxidative attack, relying on a unique thiol-based system (trypanothione) for redox balance. The nanoparticle-induced ROS flood likely overwhelms this system, causing macromolecular damage and triggering the observed apoptotic cascade. This mechanism aligns with the findings of Amani et al. (23), who reported ROS generation as a key anti-leishmanial mechanism for *C. procera* extracts. Our study thus links the green synthesis approach directly to a potent, multi-faceted cytotoxic mechanism against the parasite.

A critical advantage of any new anti-leishmanial candidate is selectivity: the ability to kill the pathogen without harming host cells. Our cytotoxicity assessment yielded highly promising results. The calculated Selectivity Index (SI), defined as CC_{50} (macrophages)/ IC_{50} (amastigotes), was substantially greater than 1 for all formulations, with the CuO NPs+ MA combination exhibiting the highest value (Table 3). This indicates a wide therapeutic window. The favorable biocompatibility is almost certainly a direct benefit of the green

http://jad.tums.ac.ir
Published Online: September 30, 2026

https://doi.org/10.18502/jad.v20i3.22579

synthesis protocol. The phytochemical corona enveloping the NPs likely modulates their interaction with mammalian cells, reducing non-specific cytotoxicity, a common drawback of nanoparticles synthesized via harsh chemical methods (25, 26). This attribute is a significant step toward addressing the core limitation of toxicity that plagues current leishmaniasis therapies (7).

This study has several limitations. The experiments were conducted using a single *L. tropica* strain and one host-cell model (THP-1-derived macrophages), which may limit the generalizability of the findings. In addition, the antileishmanial mechanisms of CuO NPs were investigated using selected oxidative stress and apoptosis markers and require further validation. Moreover, the results are restricted to in vitro conditions, and in vivo efficacy, safety, pharmacokinetics, long-term stability and batch-to-batch reproducibility of the nanoparticle formulation remain to be established.

Conclusions

In conclusion, this study describes a facile and eco-friendly method for synthesizing biocompatible CuO NPs using *C. procera* leaf extract. The resultant CuO NPs exhibit promising in vitro anti-leishmanial activity against *L. tropica*, effectively targeting both promastigote and amastigote stages. Our findings suggest that the anti-leishmanial effect may be associated with disruption of redox homeostasis and induction of apoptosis within the infected macrophage microenvironment, rather than direct parasite-specific pathway validation. Notably, the nanoparticles show additive or synergistic effects when combined with meglumine antimoniate, indicating potential for combination therapy regimens. The favorable in vitro safety profile, afforded by the green synthesis approach, highlights these nanoparticles as a promising and sustainable preclinical candidate against leishmaniasis. This work provides a robust preclinical foundation, warranting further *in vivo* efficacy studies and mechanistic exploration to advance this nanoplatform toward therapeutic application.

Acknowledgements

The authors would like to thank the Infectious Diseases and Tropical Medicine Research Center, Research Institute of Cellular and Molecular Science in Infectious Diseases, Zahedan University of Medical Sciences, Zahedan, Iran. This study was part of the MSc dissertation of Abbas Safdari Adimi (grant no. 11815) and code of ethics (IR.ZAUMS.REC.1404.090).

Conflict of interest statement

The authors declare that there is no conflict of interest.

Ethical considerations

This study was approved by the Ethics Committee of the Zahedan University of Medical Sciences (ZAUMS) and registered under the code IR.ZAUMS.REC.1404.090.

References

1. Torres-Guerrero E, Quintanilla-Cedillo MR, Ruiz-Esmenjaud J, Arenas R (2017) Leishmaniasis: a review. F1000Res. 6: 750.
2. Burza S, Croft SL, Boelaert M (2019) Leishmaniasis–authors' reply. Lancet. 393 (10174): 872–873.
3. Hadighi R, Mohebali M, Boucher P, Hajjaran H, Khamesipour A, Ouellette M (2006) Unresponsiveness to Glucantime treatment in Iranian cutaneous leishmaniasis due to drug-resistant *Leishmania tropica* parasites. PLoS Med. 3(5): e162.
4. Mohebali M, Kazemirad E, Hajjaran H, Kazemirad E, Oshaghi MA, Raoofian R, Teimouri A (2019) Gene expression analysis of antimony resistance in *Leishmania*

https://doi.org/10.18502/jad.v20i3.22579

tropica using quantitative real-time PCR focused on genes involved in trypanothione metabolism and drug transport. Arch Dermatol Res. 311(1): 9–17.
5. Hajjaran H, Azarian B, Mohebali M, Hadighi R, Assareh A, Vaziri B (2012) Comparative proteomics study on meglumine antimoniate sensitive and resistant *Leishmania tropica* isolated from Iranian anthroponotic cutaneous leishmaniasis patients. East Mediterr Health J. 18(2): 165–171.
6. Kazemi-Rad E, Mohebali M, Khadem-Erfan MB, Hajjaran H, Hadighi R, Khamesipour A (2013) Identification of antimony resistance markers in *Leishmania tropica* field isolates through a cDNA-AFLP approach. Exp Parasitol. 135(2): 344–349.
7. Ponte-Sucre A, Gamarro F, Dujardin JC, Barrett MP, López-Vélez R, García-Hernández R, Pountain AW, Mwenechanya R, Papadopoulou B (2017) Drug resistance and treatment failure in leishmaniasis: A 21st century challenge. PLoS Negl Trop Dis. 11(12): e0006052.
8. Mohtasebi S, Mohebali M, Elikaee S, Akhoundi B, Foroushani AR, Teimouri A, Yarizadeh H (2019) In vitro and in vivo anti-parasitic activity of biogenic antimony sulfide nanoparticles on *Leishmania major* (MRHO/IR/75/ER). Parasitol Res. 118(9): 2669–2678.
9. Nafari A, Cheraghipour K, Sepahvand M, Shahrokhi G, Gabal E, Mahmoudvand H (2020) Nanoparticles: new agents toward treatment of leishmaniasis. Parasite Epidemiol Control. 10: e00156.
10. Kumarasamy RV, Natarajan PM, Umapathy VR, Roy JR, Mironescu M, Palanisamy CP (2024) Clinical applications and therapeutic potentials of advanced nanoparticles: a comprehensive review on completed human clinical trials. Front Nanotechnol. 6: 1479993.
11. Jamshaid H, Din FU, Khan GM (2021) Nanotechnology based solutions for anti-leishmanial impediments: a detailed insight. J Nanobiotechnology. 19(1): 106.
12. Mehravaran A, Jaafari MR, Jalali SA, Khamesipour A, Tafaghodi M, Hojatizade M, Abbasi A, Badiee A (2015) Cationic immune stimulating complexes containing soluble *Leishmania* antigens: preparation, characterization and in vivo immune response evaluation. Iran J Immunol. 12 (4): 274–287.
13. Mehravaran A, Mirahmadi H, Akhtari J (2020) Liposomes containing the imiquimod adjuvant as a vaccine in the cutaneous leishmaniasis model. Nanomedicine J. 7 (1): 29–39.
14. Saleem K, Khursheed Z, Hano C, Anjum I, Anjum S (2019) Applications of nanomaterials in leishmaniasis: A focus on recent advances and challenges. Nanomaterials. 9(12): 1749.
15. Kanchi S, Ahmed S (2018) Green Metal Nanoparticles: Synthesis, Characterization and Their Applications. John Wiley and Sons, Hoboken, NJ.
16. Kumar P, Kumar P, Singh N, Khajuria S, Patel R, Rajana VK, Mandal D, Velayutham R (2022) Limitations of current chemotherapy and future of nanoformulation-based AmB delivery for visceral leishmaniasis–an updated review. Front Bioeng Biotechnol. 10: 1016925.
17. Naz S, Gul A, Zia M, Javed R (2023) Synthesis, biomedical applications and toxicity of CuO nanoparticles. Appl Microbiol Biotechnol. 107(4): 1039–1061.
18. Ringu T, Das A, Ghosh S, Pramanik N (2024) Exploring the potential of copper oxide nanoparticles (CuO NPs) for sustainable environmental bioengineering applications. Nanotechnol Environ Eng. 9 (4): 679–707.
19. Morsy N, Al Sherif EA, Abdel-Rassol TMA (2016) Phytochemical analysis of *Calotropis procera* with antimicrobial activity investigation. Main Group Chem. 15(3): 267–273.
20. Rani R, Sharma D, Chaturvedi M, Yadav JP (2019) Phytochemical analysis, anti-

https://doi.org/10.18502/jad.v20i3.22579

bacterial and antioxidant activity of *Calotropis procera* and *Calotropis gigantea*. Nat Prod J. 9(1): 47–60.
21. Ribeiro-Gomes FL, Sacks D (2012) The influence of early neutrophil-*Leishmania* interactions on the host immune response to infection. Front Cell Infect Microbiol. 2: 59.
22. Adejoh J, Alli LA, Okoh MP (2021) Evaluation of the anti-plasmodial potential of *Calotropis procera* latex in mice infected with *Plasmodium berghei*. MethodsX. 8: 101528.
23. Amani S, Alinejad S, Asadi N, Yousefi E, Khademvatan S, Howarth GS (2024) Anti-*Leishmania major* activity of *Calotropis procera* extract by increasing ROS production and upregulating TNF-α, IFN-γ and iNOS mRNA expression under in vitro conditions. Trop Med Health. 52(1): 16.
24. Danhalilu RL, Kankara AI, Batagarawa SM (2019) Green synthesis of metallic nanoparticles using leaf extract of *Calotropis* species and their applications: a review. Curr J Appl Sci Technol. 32(2): 1–10.
25. Adejoh J, Inyang BA, Egua MO, Nwachukwu KC, Alli LA, Okoh MP (2021) In-vivo anti-plasmodial activity of phosphate buffer extract of *Calotropis procera* latex in mice infected with *Plasmodium berghei*. J Ethnopharmacol. 277: 114237.
26. Nagime PV, Singh S, Shaikh NM, Gomare KS, Chitme H, Abdel-Wahab BA, Alqahtany YS, Khateeb MM, Habeeb MS, Bakir MB (2023) Biogenic fabrication of silver nanoparticles using *Calotropis procera* flower extract with enhanced biomimetics attributes. Materials. 16(11): 4058.
27. Ilaghi M, Sharifi I, Sharififar F, Sharifi F, Oliaee RT, Babaei Z, Shamsi-Meimandi M, Keyhani A, Bamorovat M (2021) The potential role and apoptotic profile of three medicinal plant extracts on *Leishmania tropica* by MTT assay, macrophage model and flow cytometry analysis. Parasite Epidemiol Control. 12: e00201.
28. Majeed QA, Shater AF, Alanazi AD (2023) Green synthesis, characterization and antileishmanial activity of the silver nanoparticles alone and along with meglumine antimoniate against *Leishmania major* infection. Iran J Parasitol. 18(4): 535–545.
29. Thatyana M, Dube NP, Kemboi D, Manicum ALE, Mokgalaka-Fleischmann NS, Tembu JV (2023) Advances in phytonanotechnology: A plant-mediated green synthesis of metal nanoparticles using *Phyllanthus* plant extracts and their antimicrobial and anticancer applications. Nanomaterials. 13(19): 2616.